Unsplit variables perfectly matched layers for the shallow water equations with Coriolis forces

S. Abarbanel [a], D. Stanescu [b,*] and M.Y. Hussaini [b]

[a] *Department of Mathematics, Institute of Advanced Studies, Tel Aviv University, Tel Aviv, Israel*
[b] *School of Computational Science and Information Technology, Florida State University,
Tallahassee, FL, USA*

The paper presents an analytical and numerical study of two perfectly matched layer (PML) formulations for the shallow water equations in terms of the unsplit physical variables. A perturbation method followed by a change of dependent variable allows us to extend the methods to include the Coriolis forces. The PML equations, usually given in terms of the primitive variables, are also presented here in terms of the conservative variables, which facilitates their use in flows containing discontinuities. The performance of the two methods on a set of test cases is investigated.

Keywords: nonreflecting boundary conditions, perfectly matched layers, shallow water equations

1. Introduction

Geoscience problems are naturally posed in unbounded domains. The computational domain for a discrete solution of such problems is necessarily bounded with artificial boundaries. One of the earliest examples is the limited-area/regional numerical weather forecast model where there are no natural external boundaries. Artificial boundaries require boundary conditions that ensure well-posedness of the corresponding truncated-domain problem as well as accuracy of the relevant solution with respect to the solution of the original problem in the unbounded domain. Furthermore, these artificial boundary conditions must be consistent with the discretization scheme and easily implementable. Such boundary conditions are variously known as lateral boundary conditions or transparent boundary conditions (in atmospheric science), nonreflecting boundary conditions (in aeronautical science), and radiation boundary conditions or absorbing boundary conditions (in numerical analysis and computational aeroacoustics).

A popular method of dealing with the truncated physical domain is to surround it with a zone in which non-physical equations are employed to filter, damp or convect out

---

* Currently at: Department of Mathematics, P.O. Box 3036, University of Wyoming, Laramie, WY 82071-3036, USA. E-mail: stanescu@uwyo.edu.

the incident waves so that there is little reflection into the physical domain of interest. In the geoscience literature [15,17], such a zone is usually called a sponge layer, where wave equations are employed with damping terms. In the context of electrodynamics, Berenger [4] proposed to split the governing equations (i.e., the Maxwell's equations) in the coordinate directions with additional degrees of freedom. The additional degrees of freedom are then exploited to endow the non-physical zones which he calls perfectly matching layers (PML) with the property of absorbing the incident waves irrespective of their frequency and orientation. Hu [13] extended the PML technique to the linearized Euler equations and studied the acoustic, vorticity and entropy wave propagation in the presence of uniform flow. Hayder et al. [11] applied the technique to the nonlinear Euler equations governing the problems of shock/vortex interaction, free shear layer and axisymmetric jet. They observed a weak instability in the form of three-point oscillations in the solution, which were simply removed by a low-pass filter. Hesthaven [12] showed that this weak instability is due to lack of strong well-posedness resulting from the splitting of the equations in the matched layer. Abarbanel and Gottlieb [1] placed the PML methodology on a firm mathematical basis. Subsequently, Abarbanel et al. [2] employed it to develop the first strongly well-posed PML formulation for what they call the advective acoustics problem (i.e., sound wave propagation in an otherwise uniform flow within the framework of linearized Euler equations). More recently, Hu [14] provided a new stable PML formulation, which is simpler and easier to implement, and which can also be extended to include nonuniform mean flow. Also, it can easily accommodate the equations in conservation form without splitting and can be made strongly well-posed by the addition of arbitrarily small terms.

Darblade et al. [5] and Navon et al. [18] appear to be the first to apply the PML technique to the limited-area shallow water equations, which typify a certain class of problems in atmospheric and oceanic sciences. The former study is confined to an analysis of linearized shallow water equations, while the latter is the first study of the nonlinear shallow water equations with a PML procedure. The latter study follows the original PML approach, splitting the equations in the matched layer in the coordinate directions and introducing damping terms. The equations are discretized using the Miller–Pierce finite-difference scheme. The results show that the PML approach yields better accuracy than the traditional approaches such as the characteristic boundary condition or the absorbing boundary conditions of Engquist and Majda [8,9].

The current investigation extends the state-of-the art PML methodology, namely, the procedures due to Abarbanel et al. [2], and Hu [14] to the nonlinear shallow water equations with Coriolis forces. The effect of the Coriolis forces is accounted for by the use of a perturbation technique with the Coriolis factor as a small parameter. Furthermore, the PML equations, usually formulated for linearized equations in primitive variables, are formally expressed in conservative variables. They are used both in linearized and nonlinear form in several test problems, for which the two procedures are compared with other possible lateral boundary conditions under different discretizations. Both a fourth-order finite difference method, traditionally used with PML methods, and

a spectral multidomain method, which is attracting increasing attention [6,7,10,19] due to its accuracy properties, are used for this purpose.

2. Analysis of governing equations

The two-dimensional shallow water equations, including the effect of the Coriolis forces, can be written as

$$
\begin{aligned}
\frac{\partial h}{\partial t} + u\frac{\partial h}{\partial x} + v\frac{\partial h}{\partial y} + h\left(\frac{\partial u}{\partial x} + \frac{\partial v}{\partial y}\right) &= 0, \\
\frac{\partial u}{\partial t} + u\frac{\partial u}{\partial x} + v\frac{\partial u}{\partial y} + g\frac{\partial h}{\partial x} - fv &= 0, \\
\frac{\partial v}{\partial t} + u\frac{\partial v}{\partial x} + v\frac{\partial v}{\partial y} + g\frac{\partial h}{\partial y} + fu &= 0,
\end{aligned}
\tag{1}
$$

where h is the fluid height, g the gravitational constant, f the Coriolis factor and u and v the x- and y-components of the fluid velocity, respectively. In terms of the potential $\phi = gh$, the equations become

$$
\begin{aligned}
\frac{\partial \phi}{\partial t} + u\frac{\partial \phi}{\partial x} + v\frac{\partial \phi}{\partial y} + \phi\left(\frac{\partial u}{\partial x} + \frac{\partial v}{\partial y}\right) &= 0, \\
\frac{\partial u}{\partial t} + u\frac{\partial u}{\partial x} + v\frac{\partial u}{\partial y} + \frac{\partial \phi}{\partial x} - fv &= 0, \\
\frac{\partial v}{\partial t} + u\frac{\partial v}{\partial x} + v\frac{\partial v}{\partial y} + \frac{\partial \phi}{\partial y} + fu &= 0
\end{aligned}
\tag{2}
$$

or, equivalently,

$$
\frac{\partial V}{\partial t} + \tilde{A}\frac{\partial V}{\partial x} + \widetilde{B}\frac{\partial V}{\partial y} + f\widetilde{C}V = 0,
\tag{3}
$$

where $V = (\phi\ u\ v)^{\mathrm{T}}$ and $\tilde{A}$, $\widetilde{B}$, and $\widetilde{C}$ are the following 3×3 matrices

$$
\tilde{A} = \begin{bmatrix} u & \phi & 0 \\ 1 & u & 0 \\ 0 & 0 & u \end{bmatrix}, \qquad \widetilde{B} = \begin{bmatrix} v & 0 & \phi \\ 0 & v & 0 \\ 1 & 0 & v \end{bmatrix}, \qquad \widetilde{C} = \begin{bmatrix} 0 & 0 & 0 \\ 0 & 0 & -1 \\ 0 & 1 & 0 \end{bmatrix}.
\tag{4}
$$

For the following analysis, as well as for the purpose of numerical discretization, it is useful to first non-dimensionalize these equations. To this end, let us choose the following reference values: a length scale specific to the problem, denoted by H_{r}, for the spatial coordinates x and y, a reference velocity $u_{\mathrm{r}} = \sqrt{gH_{\mathrm{r}}}$ for the two velocity components, a reference potential $\phi_{\mathrm{r}} = u_{\mathrm{r}}^2$ for the potential and a reference time $t_{\mathrm{r}} = H_{\mathrm{r}}/u_{\mathrm{r}}$ for time. The Coriolis factor is non-dimensionalized with $f_{\mathrm{r}} = u_{\mathrm{r}}/H_{\mathrm{r}}$. With this choice, the equations for the corresponding non-dimensional quantities remain the same as equations (2). In the rest of the paper we work only with non-dimensional variables, keeping the same notation as for the dimensional ones for simplicity.

The main difficulty in obtaining an extension of the PML methods as devised for electromagnetics and acoustics to the case of the shallow water equations resides in the presence of the coupling source terms due to the Coriolis forces. Since the maximum value of the non-dimensional Coriolis factor is approximately $f = 1.5 \times 10^{-3}$ for a reference length $H_r = 1$ km, we can proceed by using a perturbation procedure with the non-dimensional Coriolis factor f as the small parameter. Hence, the solution is considered to be, to a good approximation, given by

$$V = \begin{pmatrix} \phi \\ u \\ v \end{pmatrix} = V_0 + f V_1 + f^2 V_2 + \cdots. \tag{5}$$

Introducing this expression in the governing equations and retaining terms to the zeroth-order yields

$$
\begin{aligned}
&\frac{\partial \phi_0}{\partial t} + u_0 \frac{\partial \phi_0}{\partial x} + v_0 \frac{\partial \phi_0}{\partial y} + \phi_0 \left(\frac{\partial u_0}{\partial x} + \frac{\partial v_0}{\partial y} \right) = 0, \\
&\frac{\partial u_0}{\partial t} + u_0 \frac{\partial u_0}{\partial x} + v_0 \frac{\partial u_0}{\partial y} + \frac{\partial \phi_0}{\partial x} = 0, \\
&\frac{\partial v_0}{\partial t} + u_0 \frac{\partial v_0}{\partial x} + v_0 \frac{\partial v_0}{\partial y} + \frac{\partial \phi_0}{\partial y} = 0.
\end{aligned}
\tag{6}
$$

A solution to this problem is given by $v_0 = 0$, $\phi_0 = 1$, and $u_0 = \text{const} = F_0$, where F denotes the Froude number, $F = u/u_r$.

The equations governing the first order perturbation (first order terms in f) are

$$
\begin{aligned}
&\frac{\partial \phi_1}{\partial t} + u_0 \frac{\partial \phi_1}{\partial x} + v_0 \frac{\partial \phi_1}{\partial y} + u_1 \frac{\partial \phi_0}{\partial x} + v_1 \frac{\partial \phi_0}{\partial y} \\
&\quad + \phi_0 \left(\frac{\partial u_1}{\partial x} + \frac{\partial v_1}{\partial y} \right) + \phi_1 \left(\frac{\partial u_0}{\partial x} + \frac{\partial v_0}{\partial y} \right) = 0, \\
&\frac{\partial u_1}{\partial t} + u_0 \frac{\partial u_1}{\partial x} + v_0 \frac{\partial u_1}{\partial y} + u_1 \frac{\partial u_0}{\partial x} + v_1 \frac{\partial u_0}{\partial y} + \frac{\partial \phi_1}{\partial x} - v_0 = 0, \\
&\frac{\partial v_1}{\partial t} + u_0 \frac{\partial v_1}{\partial x} + v_0 \frac{\partial v_1}{\partial y} + u_1 \frac{\partial v_0}{\partial x} + v_1 \frac{\partial v_0}{\partial y} + \frac{\partial \phi_1}{\partial y} + u_0 = 0.
\end{aligned}
\tag{7}
$$

Using the solution to the zeroth-order problem, they become

$$
\begin{aligned}
&\frac{\partial \phi_1}{\partial t} + F_0 \frac{\partial \phi_1}{\partial x} + \left(\frac{\partial u_1}{\partial x} + \frac{\partial v_1}{\partial y} \right) = 0, \\
&\frac{\partial u_1}{\partial t} + F_0 \frac{\partial u_1}{\partial x} + \frac{\partial \phi_1}{\partial x} = 0, \\
&\frac{\partial v_1}{\partial t} + F_0 \frac{\partial v_1}{\partial x} + \frac{\partial \phi_1}{\partial y} + F_0 = 0.
\end{aligned}
\tag{8}
$$

This form of the equations does not allow a straightforward application of the PML technique due to the presence of the coupling term F_0 in the last equation. In

order to eliminate this coupling term, we introduce the change of variable $w_1(x, y, t) = v_1(x, y, t) + x$, thus obtaining

$$\frac{\partial \phi_1}{\partial t} + F_0 \frac{\partial \phi_1}{\partial x} + \left(\frac{\partial u_1}{\partial x} + \frac{\partial w_1}{\partial y} \right) = 0,$$

$$\frac{\partial u_1}{\partial t} + F_0 \frac{\partial u_1}{\partial x} + \frac{\partial \phi_1}{\partial x} = 0, \tag{9}$$

$$\frac{\partial w_1}{\partial t} + F_0 \frac{\partial w_1}{\partial x} + \frac{\partial \phi_1}{\partial y} = 0.$$

These equations are identical to the linearized Euler equations governing the propagation of acoustic waves in a uniform mean flow, as given, for example, in [2]. We will work with these equations to develop PML methods that can be applied eventually to equations (2).

3. PML methods

3.1. Equations in transformed variables

This section presents two PML approaches for the set of equations (9). The first one results directly from the work of Hu [14]. For ease of presentation, let us write the equations as

$$\frac{\partial U}{\partial t} + A \frac{\partial U}{\partial x} + B \frac{\partial U}{\partial y} = 0, \tag{10}$$

where $U = (\phi_1 \ u_1 \ w_1)^{\mathrm{T}}$ and A and B are 3×3 matrices given by

$$A = \begin{bmatrix} F_0 & 1 & 0 \\ 1 & F_0 & 0 \\ 0 & 0 & F_0 \end{bmatrix}, \qquad B = \begin{bmatrix} 0 & 0 & 1 \\ 0 & 0 & 0 \\ 1 & 0 & 0 \end{bmatrix}. \tag{11}$$

A straightforward extension of the analysis presented by Hu [14] to this system of equations yields the following PML equations

$$\frac{\partial U}{\partial t} + A \frac{\partial U}{\partial x} + B \frac{\partial U}{\partial y} + \sigma_y A \frac{\partial q}{\partial x} + \sigma_x B \frac{\partial q}{\partial y} + (\sigma_x + \sigma_y)U$$

$$+ \sigma_x \sigma_y q + \frac{\sigma_x F_0}{1 - F_0^2} A(U + \sigma_y q) = 0, \tag{12}$$

$$\frac{\partial q}{\partial t} + \varepsilon \sigma_y A \frac{\partial U}{\partial x} + \varepsilon \sigma_y B \frac{\partial U}{\partial y} = U.$$

Here q is an auxiliary variable needed only in the PML domain, ε is an arbitrarily small parameter needed to ensure strong well-posedness and σ_x and σ_y are the absorption coefficients in the x- and y-layers, respectively. The plane wave solutions of this system can be shown to be perfectly matched to the solutions of the set of equations (10) for $\varepsilon = 0$.

The second PML approach considered here is the one proposed by Abarbanel et al. [2]. In this case, the PML equations are

$$
\frac{\partial \phi_1}{\partial t} + F_0 \frac{\partial \phi_1}{\partial x} + \frac{\partial u_1}{\partial x} + \frac{\partial w_1}{\partial y} = -\sigma_x \phi_1 - \sigma_x F_0 u_1 - \mu_y \phi_1,
$$

$$
\frac{\partial u_1}{\partial t} + F_0 \frac{\partial u_1}{\partial x} + \frac{\partial \phi_1}{\partial x} = -\sigma_x u_1 - \sigma_x F_0 \phi_1 - \mu_y u_1,
$$

$$
\frac{\partial w_1}{\partial t} + F_0 \frac{\partial w_1}{\partial x} + \frac{\partial \phi_1}{\partial y} = -\sigma_x w_1 + 2\sigma_x Q_x + \sigma_x^2 R_x + F_0 \sigma_x' P_x
$$

$$
\qquad\qquad - \varepsilon_x w_1 + 2\sigma_y Q_y + \sigma_y^2 R_y + \sigma_y' P_y + 2\mu_y Q_y,
$$

$$
\frac{\partial Q_x}{\partial t} = -\left(1 - F_0^2\right)\frac{\partial \phi}{\partial y}, \tag{13}
$$

$$
\frac{\partial P_x}{\partial t} = \left(1 - F_0^2\right)(\phi_1 - \sigma_y P_y),
$$

$$
\frac{\partial R_x}{\partial t} = \left(1 - F_0^2\right)(Q_x - \mu_x R_x),
$$

$$
\frac{\partial Q_y}{\partial t} = \left(1 - F_0^2\right)\left(\frac{\partial \phi_1}{\partial y} - 2\sigma_y Q_y - \sigma_y^2 R_y - \sigma_y' P_y - \mu_y Q_y\right),
$$

$$
\frac{\partial P_y}{\partial t} = \left(1 - F_0^2\right)(\phi_1 - \sigma_y P_y), \qquad \frac{\partial R_y}{\partial t} = \left(1 - F_0^2\right)(Q_y - \mu_y R_y).
$$

Six auxiliary variables have been introduced here, namely Q_x, P_x, R_x, Q_y, P_y, R_y. The damping parameters are denoted again by σ_x and σ_y, while the remaining parameters, introduced to stabilize the PML equations, are taken as

$$
\varepsilon_x(x) = \sqrt{F_0 |\sigma_x'(x)|}, \qquad \mu_x(x) = \sigma_x(x), \qquad \mu_y(x) = \sigma_y(y). \tag{14}
$$

3.2. Original variables

From the above equations one can easily obtain the PML formulation in the original variables. To keep the paper within a reasonable length, we present here only the development for equations (12). As $w_1 = v_1 + x$, the system can be written

$$
\frac{\partial V_1}{\partial t} + A\left(\frac{\partial V_1}{\partial x} + e_v\right) + B\frac{\partial V_1}{\partial y} + \sigma_y A \frac{\partial q}{\partial x} + \sigma_x B \frac{\partial q}{\partial y}
$$

$$
+ (\sigma_x + \sigma_y)(V_1 + x e_v) + \sigma_x \sigma_y q + \frac{\sigma_x F_0}{1 - F_0^2} A(V_1 + x e_v + \sigma_y q) = 0, \tag{15}
$$

$$
\frac{\partial q}{\partial t} + \varepsilon \sigma_y A\left(\frac{\partial V_1}{\partial x} + e_v\right) + \varepsilon \sigma_y B \frac{\partial V_1}{\partial y} = V_1 + x e_v,
$$

where $V_1 = (\phi_1\ u_1\ v_1)^{\mathrm{T}}$ and $e_v = (0\ 0\ 1)^{\mathrm{T}}$. These PML equations can thus be used for the linearized shallow water equations in the presence of Coriolis forces. To obtain a PML method for the nonlinear equations, we multiply the above equations by f and add

the result to the zeroth order equations. After careful identification of the total variables, we propose the following system of equations for the nonlinear case

$$
\frac{\partial V}{\partial t} + \tilde{A}\frac{\partial V}{\partial x} + \tilde{B}\frac{\partial V}{\partial y} + f\tilde{C}V + \sigma_y\tilde{A}\frac{\partial q}{\partial x} + \sigma_x\tilde{B}\frac{\partial q}{\partial y}
$$
$$
+ (\sigma_x + \sigma_y)(V' + fxe_v) + \sigma_x\sigma_y q + \frac{\sigma_x F_0}{1 - F_0^2}\tilde{A}(V' + fxe_v + \sigma_y q) = 0, \qquad (16)
$$
$$
\frac{\partial q}{\partial t} + \varepsilon\sigma_y\tilde{A}\left(\frac{\partial V}{\partial x} + e_v\right) + \varepsilon\sigma_y\tilde{B}\frac{\partial V}{\partial y} = V' + fxe_v,
$$

where $V' = V - V_0$ is the total mean flow perturbation.

4. Conservative form

For numerical methods based on the conservative form of the shallow water equations, the PML equations are not easy to implement in the form presented above which uses the primitive variables vector V. To devise a suitable implementation in this case, denote by $S = (\phi\ m\ n)^{\mathrm{T}}$ the conserved variables vector, with $m = \phi u$ and $n = \phi v$. Let

$$
M = \frac{\partial S}{\partial V} = \begin{bmatrix} 1 & 0 & 0 \\ u & \phi & 0 \\ v & 0 & \phi \end{bmatrix} \qquad (17)
$$

be the transformation matrix between the conservative and the primitive variables, where the variables now represent the full quantities, not only the perturbation. The shallow water equations (ignoring the Coriolis forces as they do not introduce any complication and can be added later) can be written in terms of the conserved variables either in conservation form

$$
\frac{\partial S}{\partial t} + \frac{\partial F}{\partial x} + \frac{\partial G}{\partial y} = 0, \qquad (18)
$$

where the x- and y-fluxes are given by

$$
F = \begin{bmatrix} m \\ \dfrac{m^2}{\phi} + \dfrac{\phi^2}{2} \\ \dfrac{mn}{\phi} \end{bmatrix}, \qquad G = \begin{bmatrix} n \\ \dfrac{mn}{\phi} \\ \dfrac{n^2}{\phi} + \dfrac{\phi^2}{2} \end{bmatrix}, \qquad (19)
$$

or in the so-called quasi-linear form

$$
\frac{\partial S}{\partial t} + \alpha\frac{\partial S}{\partial x} + \beta\frac{\partial S}{\partial y} = 0, \qquad (20)
$$

where the Jacobian matrices are given by

$$
\alpha = \frac{\partial F}{\partial S} = \begin{bmatrix} 0 & 1 & 0 \\ \phi - \dfrac{m^2}{\phi^2} & \dfrac{2m}{\phi} & 0 \\ -\dfrac{mn}{\phi^2} & \dfrac{n}{\phi} & \dfrac{m}{\phi} \end{bmatrix}, \qquad \beta = \frac{\partial G}{\partial S} = \begin{bmatrix} 0 & 0 & 1 \\ -\dfrac{mn}{\phi^2} & \dfrac{n}{\phi} & \dfrac{m}{\phi} \\ \phi - \dfrac{n^2}{\phi^2} & 0 & \dfrac{2n}{\phi} \end{bmatrix}. \quad (21)
$$

Identifying the conservative form of the equations with the primitive-variables form (excluding Coriolis terms), one can readily obtain the following relations

$$
\tilde{A} = M^{-1}\alpha M, \qquad \widetilde{B} = M^{-1}\beta M. \quad (22)
$$

We discuss here the development of the PML equations in conservative variables for the set of equations (16), as the other set can be obtained in a similar fashion. The first equation in the set can be written in the case $f = 0$ as

$$
M^{-1}\frac{\partial S}{\partial t} + \tilde{A}M^{-1}\frac{\partial S}{\partial x} + \widetilde{B}M^{-1}\frac{\partial S}{\partial y} + \sigma_y\tilde{A}\frac{\partial q}{\partial x} + \sigma_x\widetilde{B}\frac{\partial q}{\partial y}
$$
$$
+ (\sigma_x + \sigma_y)V' + \sigma_x\sigma_y q + \frac{\sigma_x F_0}{1 - F_0^2}\tilde{A}(V' + \sigma_y q) = 0. \quad (23)
$$

Multiplying by M, one notices that the first three terms in this equation are identical to the conservative equations (20). Moreover, these equations hold not only for the full variables but also for the perturbations, as the full variables can be written in the PML region as $S = S_0 + S'$ where S_0 implicitly satisfies the steady form of the equations. Since for small perturbations $S' = MV$, we obtain

$$
\frac{\partial S'}{\partial t} + \alpha\frac{\partial S'}{\partial x} + \beta\frac{\partial S'}{\partial y} + \sigma_y M\tilde{A}\frac{\partial q}{\partial x} + \sigma_x M\widetilde{B}\frac{\partial q}{\partial y}
$$
$$
+ (\sigma_x + \sigma_y)S' + \sigma_x\sigma_y Mq + \frac{\sigma_x F_0}{1 - F_0^2}\alpha(S' + \sigma_y Mq) = 0. \quad (24)
$$

Because the mean flow is supposed to be uniform in the PML region, M can be considered constant. Multiplying the second equation in (16) by M and performing some manipulation, we obtain the following PML equations in conservative variables:

$$
\frac{\partial S}{\partial t} + \alpha\frac{\partial S}{\partial x} + \beta\frac{\partial S}{\partial y} + \sigma_y\alpha\frac{\partial q}{\partial x} + \sigma_x\beta\frac{\partial q}{\partial y}
$$
$$
+ (\sigma_x + \sigma_y)S' + \sigma_x\sigma_y q + \frac{\sigma_x F_0}{1 - F_0^2}\alpha(S' + \sigma_y q) = 0, \quad (25)
$$
$$
\frac{\partial q}{\partial t} + \varepsilon\sigma_y\alpha\frac{\partial S}{\partial x} + \varepsilon\sigma_y\beta\frac{\partial S}{\partial y} = S',
$$

where we keep the same notation for the auxiliary variable q, which is however updated from a different equation in this case.

5. Numerical study

5.1. Discretization methods

The proposed PML equations have been tested using several different discretizations. To make the paper self-contained, this section succinctly presents the methods that we used. The nonlinear conservative form of the equations was discretized with a multidomain Chebyshev method first proposed by Kopriva and Kolias [16]. In this case the computational domain is partitioned into a number of subdomains ("elements" henceforth), and on each element the solution is approximated as a tensor product of polynomials in each of the space coordinates,

$$S(x, y, t) = \sum_{i=1}^{N} \sum_{j=1}^{N} S(x_i, y_j, t) h_i(x) h_j(y), \tag{26}$$

where the points x_i and y_j are the Gauss–Gauss quadrature points, located inside the element, and $h(x)$ is the Lagrange interpolant based on these points,

$$h_i(x) = \prod_{p=1, p \neq i}^{N} \left(\frac{x - x_p}{x_i - x_p} \right). \tag{27}$$

The values of the solution $S(x_i, y_j, t)$ are the degrees of freedom of the discretization, and N is the degree of the highest polynomial in the approximation. For a given partition of the computational domain, the accuracy of the solution increases exponentially with N if the time discretization errors are small enough. As continuity of the solution at element boundaries is not implicit in the form of the solution given above, it is explicitly enforced as part of the discretization process. To this end, one computes first the value of the interpolant (26) at the Gauss–Lobatto quadrature points $(\bar{x}_m, y_j), (x_i, \bar{y}_n), m, n = 0, \ldots, N$, which are located on the element edges (but not at element corners). For example, at points $y = y_j = $ constant the flux component F is needed and can be computed by evaluating pointwise the solution interpolant

$$S(\bar{x}_m, y, t) = \sum_{i=1}^{N} \sum_{j=1}^{N} S(x_i, y_j, t) h_i(\bar{x}_m) h_j(y), \quad m = 0, \ldots, N. \tag{28}$$

For those Gauss–Lobatto points located on the element edges there will be two flux values, one from each of the two elements which have that edge in common. A unique value is computed from these flux values using a Riemann solver [3] and is assigned to both elements. This ensures weak continuity of the solution, and the necessary flux derivatives can be evaluated by differentiating within each element the flux interpolant through the Gauss–Lobatto points

$$F(x, y, t) = \sum_{m=0}^{N} \sum_{j=1}^{N} F(\bar{x}_m, y_j, t) \bar{h}_m(x) h_j(y), \quad m = 0, \ldots, N, \tag{29}$$

where $\bar{h}$ are the Lagrange interpolants through the Gauss–Lobatto points. This differentiation can be expressed, and is actually implemented in the computer code, as a matrix–vector multiplication operation of the form

$$\{F_x\} = [D]\{F\}, \tag{30}$$

where $\{F_x\}$ is the vector of flux derivative values at the Gauss–Gauss points, $\{F\}$ is the vector of pointwise flux values at the Gauss–Lobatto points, and D is an $N \times (N + 1)$ differentiation matrix. For the boundary condition at the outer limit of the PML domain, it is straightforward under this discretization to use characteristic boundary conditions, as they can be imposed using the same Riemann solver. After computation of flux derivatives, the system of partial differential equations reduces to a system of ordinary differential equations for the degrees of freedom which are integrated in time using a low-storage Runge–Kutta method [20].

We also tested a finite difference discretization of both the nonlinear and linear equations. The dispersion relation preserving (DRP) [21] fourth order method was used for discretization in space in this case, and a linear multistep method for time integration. The degrees of freedom are the solution values q_{ij} at the nodes (i, j) of a Cartesian grid, and the finite difference approximation to the derivatives is given by

$$\left(\frac{\partial q}{\partial x}\right)_{ij} = \frac{1}{\Delta x} \sum_{m=-3}^{3} a_m q_{i+m,j}, \tag{31}$$

where $a_i = -a_{-i}$, $a_0 = 0$, $a_1 = 0.79927$, $a_2 = -0.18941$ and $a_3 = 0.02651$ in the interior of the domain [21]. Nonsymmetric finite difference stencils are used at the boundaries. Under this discretization we used either the asymptotic form of the radiation and outflow boundary conditions for the shallow water equations without the Coriolis force at the outer limit of the PML domain, or a simple closure similar to that proposed by Hu [14]. In the former case, for the points located at the boundary of the domain, a different partial differential equation is used as closure. For example, for those boundaries where the mean flow velocity is directed inside the computational domain, these equations can be written in the form (usually known as a radiation boundary condition):

$$\left(\frac{1}{V_\theta}\frac{\partial}{\partial t} + \frac{\partial}{\partial r} + \frac{1}{2r}\right)q = 0, \tag{32}$$

where $V_\theta = F_0 \cos\theta + \sqrt{1 - F_0^2 \sin^2\theta}$, with r the radius from the source of disturbance to the boundary point and θ the angle between this radius and the mean-flow velocity direction. In the latter case, denoting the entire computational domain by $[x_m, x_M] \times [y_m, y_M]$, we impose

$$\begin{aligned} \phi &= \phi_0 \quad \text{at } x = x_M, \ y = y_m, \ y = y_M, \\ \phi &= \phi_0, \qquad v = v_0 \quad \text{at } x = x_m. \end{aligned} \tag{33}$$

The damping coefficients used in the computation are of the form

$$\sigma_x(x) = \sigma_M \left| \frac{x - x_d}{L} \right|^p, \qquad \sigma_y(y) = \sigma_M \left| \frac{y - y_d}{L} \right|^p, \tag{34}$$

where the subscript d denotes the value of the respective coordinate where the PML region starts, σ_M is a constant, and p is an integer exponent. The particular values used for these parameters are specified for each computation in the next section. The value of the strong well-posedness coefficient ε is equal to zero unless otherwise mentioned. In all cases, the error was computed by comparison to a reference solution obtained on a domain large enough to remain unaffected by reflections until the final time of the computation. In order to study the stability of the proposed PML formulations, no filtering of any kind has been used to stabilize the computations in the domain proper or in the PML region, even in the nonlinear case.

5.2. Flows without Coriolis forces

5.2.1. Gaussian pulses

The first tests investigated the propagation of potential and vorticity pulses specified initially by

$$\begin{aligned}
\phi(x, y, t = 0) &= \phi_0 + A_\phi e^{-\ln(2)((x+x_\phi)^2 + y^2)/\delta_\phi^2}, \\
u(x, y, t = 0) &= u_0 + A_v y e^{-\ln(2)((x+x_v)^2 + y^2)/\delta_v^2}, \\
v(x, y, t = 0) &= v_0 - A_v(x - x_v) e^{-\ln(2)((x+x_v)^2 + y^2)/\delta_v^2}.
\end{aligned} \tag{35}$$

Here $\delta_\phi = 3$ represents the width of the potential pulse, and $\delta_v = 4$ the width of the vorticity pulse. Results for $F_0 = 0$, $A_v = 0$, $A_\phi = 0.1$ and $x_\phi = 0$ have been computed using both the spectral method with 25 elements and the solution interpolated by a polynomial of degree twelve on each element, and the finite difference method with a step size $\Delta x = \Delta y = 1$. The computational domain is $[-45, 45]^2$, with a PML domain of width $L = 10$ positioned inside. In both cases the exponent for the damping profile was set to $p = 2$, and $\sigma_M = 1$. Figure 1 shows the maximum error in the potential ϕ at the interior limit of the PML domain for the nonlinear conservative formulation using the spectral discretization. Unfortunately the second PML formulation (13) turned out to be unstable, due to discontinuities of the order of interpolation error that exist at interdomain boundaries in this discretization, so we can only report results using the first PML formulation (PML1, equation (12)). The reflections produced by the characteristic boundary treatment are about two orders of magnitude larger than those generated by PML1. In figure 2 we plot again the maximum error in the potential computed using the linear equations discretized by the finite difference method when the computational domain is closed by the simple boundary conditions in equation (33), and in figure 3 we use the asymptotic boundary condition. The reflections caused by the simple boundary condition are significantly reduced by both PML formulations, i.e. about five times by PML2 and with more than two orders of magnitude by PML1. Note that the presence of
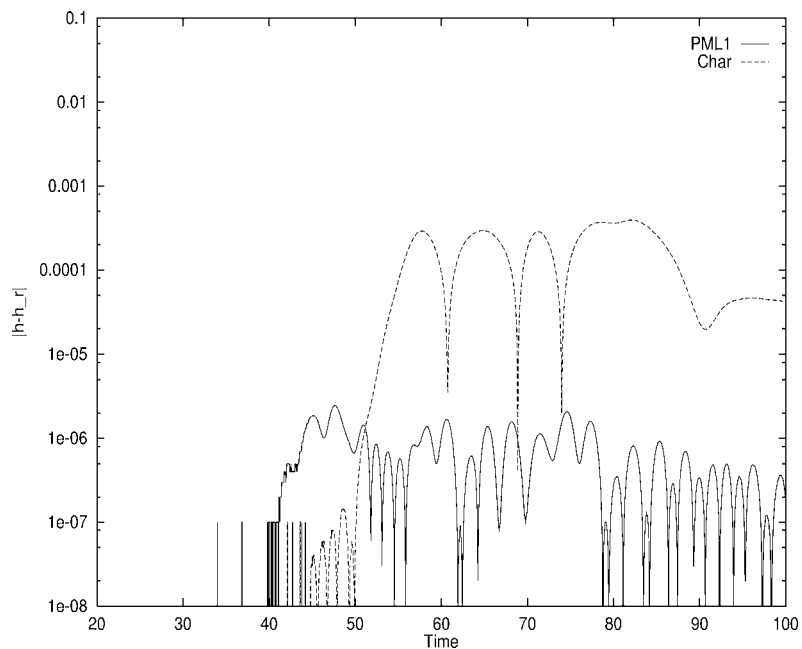
Figure 1. Maximum error in the potential for the propagation of a Gaussian pulse at $F_0 = 0.0$, nonlinear conservative formulation, spectral multidomain method. PML versus characteristic boundary conditions.
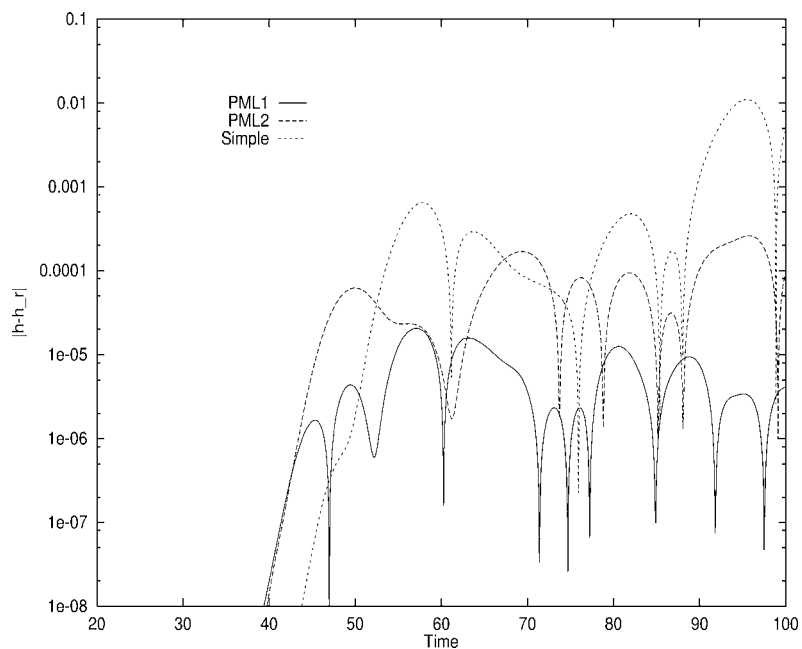
Figure 2. Maximum error in the potential for the propagation of a Gaussian pulse at $F_0 = 0.0$, linear primitive variables formulation, finite difference method. PML versus simple boundary conditions.
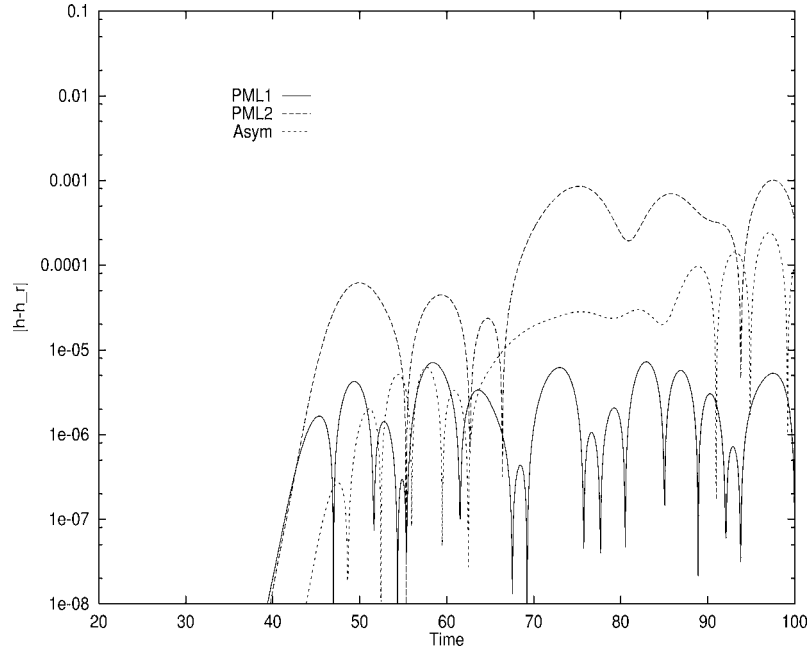
Figure 3. Maximum error in the potential for the propagation of a Gaussian pulse at $F_0 = 0.0$, linear primitive variables formulation, finite difference method. PML versus asymptotic boundary conditions.

the layers causes reflections to develop sooner (at approximately $t = 40$) in the results than for the cases with no layer. The asymptotic boundary condition is quite accurate, to the extent that formulation (13) (PML2) is not able to outperform it, while PML1 reduces the reflections by more than one order of magnitude.

As a more demanding test case, we consider $A_\phi = 0.1$, $x_\phi = -20$, $A_v = 0.005$ and $x_v = 25$, and run the nonlinear finite difference method with a layer width $L = 15$, $\sigma_M = 1$ and $p = 4$. In this case the mean flow Froude number is $F_0 = 0.2$. Figure 4 shows the maximum error in the x-velocity component along the right boundary of the domain proper as a function of time with different boundary conditions. In this case PML1 is more than an order of magnitude better than the asymptotic boundary condition, which still performs better than PML2.

5.2.2. Pulsating source

As a test of the long-time integration properties of the PML algorithms, we consider as a second test the propagation of gravity waves generated by a harmonic source in a uniform mean flow. The following source term is added to the right-hand side of the equation for the potential

$$\mathcal{R}(x, y, t) = A_\phi e^{-\ln(2)(x^2+y^2)/\delta_\phi^2} \sin(\omega t). \tag{36}$$

We set $F_0 = 0.3$, $A_\phi = 0.01$, $\delta_\phi = 3$ and $\omega = 0.2$ and compare the solution obtained in a large reference domain with the solution obtained in a computational domain $[-55, 55]^2$
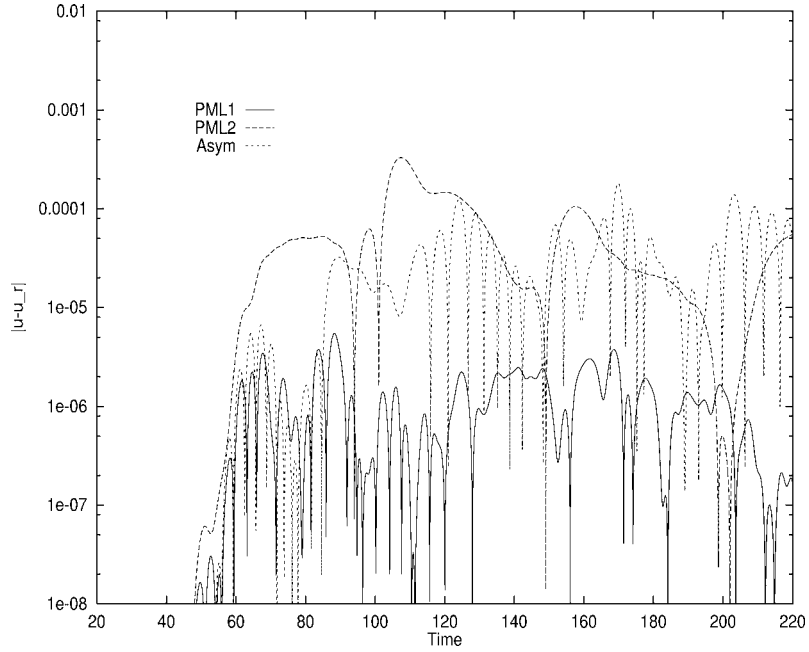
Figure 4. Maximum error in u for propagation of Gaussian pulses at $F_0 = 0.2$, nonlinear nonconservative formulation, finite difference method. PML versus asymptotic boundary conditions.
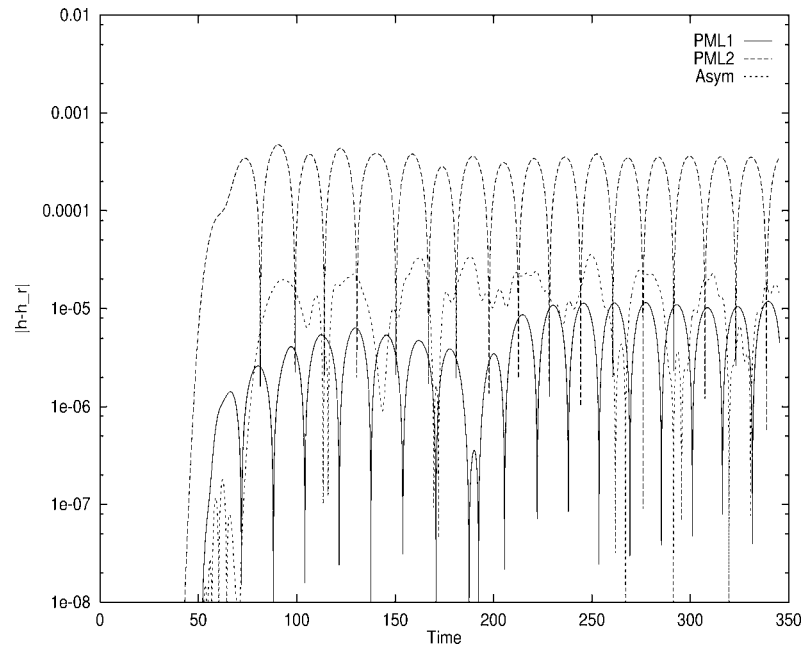
Figure 5. Maximum error in ϕ for source in $F_0 = 0.3$ flow, linear primitive variables formulation, finite difference method. PML versus asymptotic boundary conditions.

Level	phi
15	9.500E-03
14	7.504E-03
13	5.509E-03
12	3.514E-03
11	1.519E-03
10	-4.767E-04
9	-2.472E-03
8	-4.467E-03
7	-6.463E-03
6	-8.458E-03
5	-1.045E-02
4	-1.245E-02
3	-1.444E-02
2	-1.644E-02
1	-1.843E-02
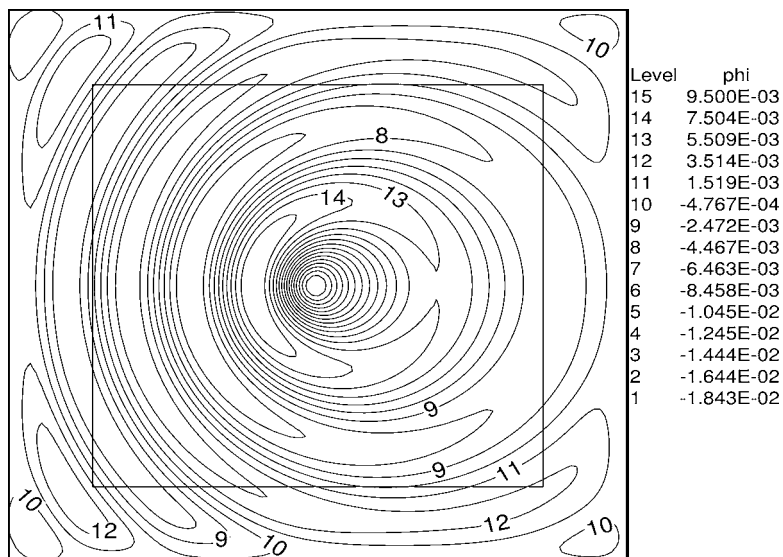
Figure 6. Contour levels for the potential ϕ, source in $F_0 = 0.3$ flow, PML1.
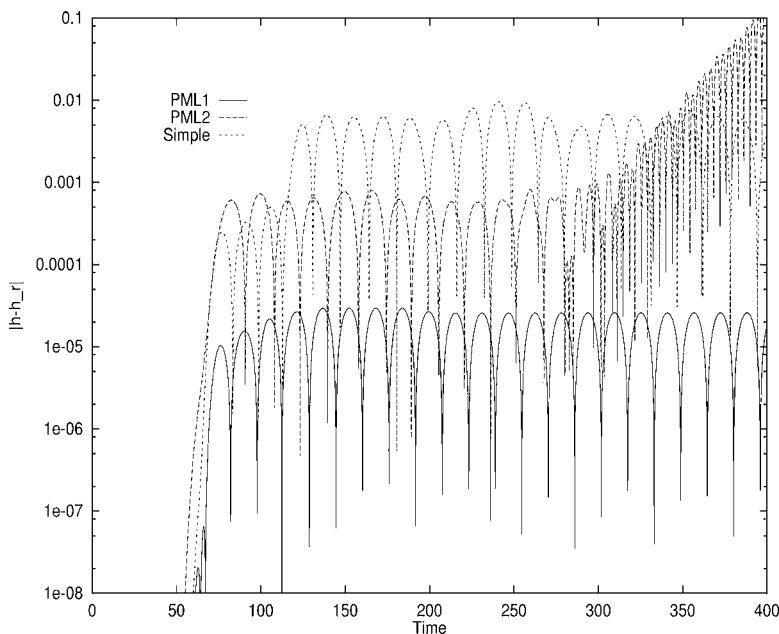
Figure 7. Maximum error in ϕ for harmonic source at $F_0 = 0$ flow, linear primitive variables formulation, finite difference method. PML versus simple boundary conditions.

using a PML region of width 15 positioned inside. The parameters for damping in the PML are again taken as $\sigma_M = 1$ and $p = 4$. Figure 5 presents the maximum error in the potential at $x = 39$ as a function of time for the PML methods closed with the

(a)

(b)
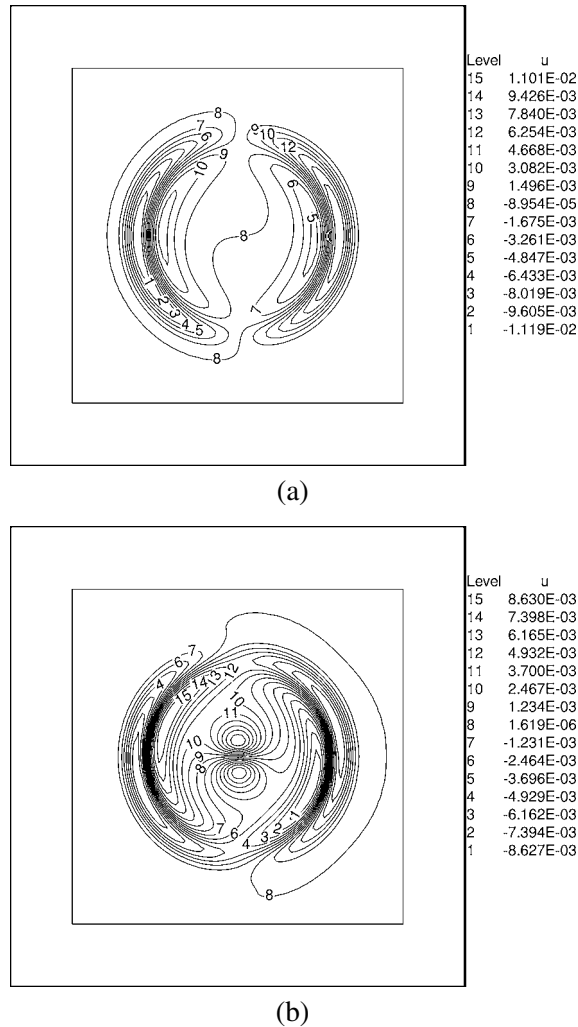
Figure 8. *x*-velocity (*u*) contours at $t = 23$ for propagation of a Gaussian pulse at $F_0 = 0.01$, for
(a) $f = 0.01$ and (b) $f = 0.1$.

asymptotic boundary condition. In this advective case both methods showed no sign of
instability. A contour plot of the potential values at time $t = 100$ is shown in figure 6.
We noticed however that in the absence of mean flow, i.e., for $F_0 = 0$, PML2 became
unstable, as can be seen in figure 7 for times later than $t = 300$.

5.3. Flows with Coriolis forces

For this type of flow we only performed numerical studies using the linear equa-
tions. The results pertaining to the performance of the two PML formulations presented
in the previous section extend naturally to this case, since the computations can be done

(a)

(b)
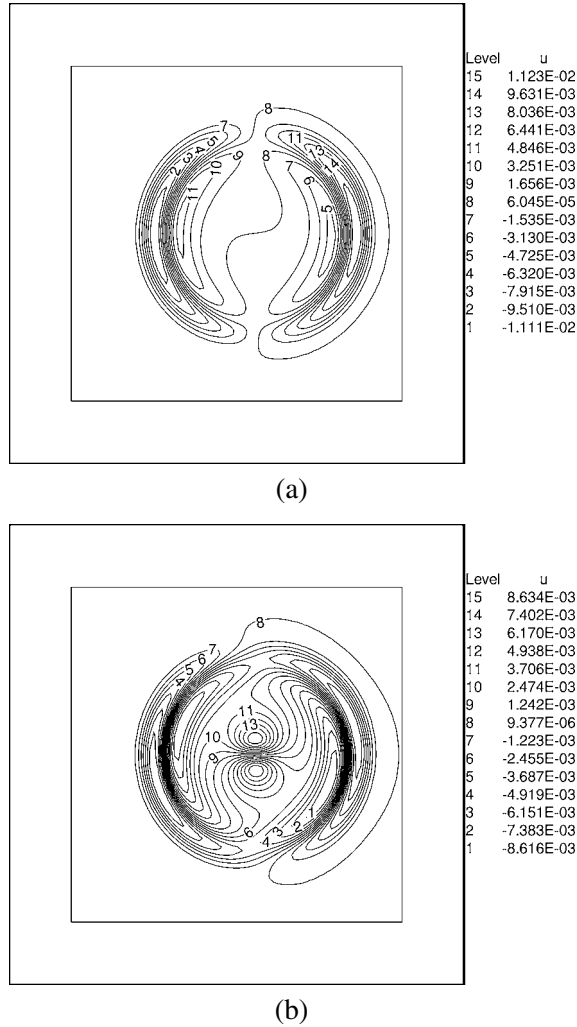
Figure 9. x-velocity (u) contours at $t = 23$ for propagation of a Gaussian pulse at $F_0 = 0.2$, for
(a) $f = 0.01$ and (b) $f = 0.1$.

using the newly introduced variable $w_1 = v_1 + x$, and the results for v can then be re-
covered afterwards by setting $v = v_0 + f(w_1 - x)$. We note that in the nonlinear case
one needs to work with the original variables directly. To show the effect of the Coriolis
force on the performance of the damping layer, we consider the propagation of a pulse as
given in equation (35), with $\delta_\phi = 3$, $A_\phi = 0.1$, $x_\phi = 0$ and $A_v = 0$, and compute the so-
lution in the domain $[-55, 55]^2$, with a PML domain of width $L = 15$ positioned inside
for different values of the Coriolis force and different values of the Froude number F_0.
The values of the damping parameters are taken as $\sigma_M = 1$ and $p = 2$, and only PML1
was tested for this case. By extension, we still use at the outer limit of the PML domain
the asymptotic type boundary condition [21]. Shown in figure 8 are the contours for u at
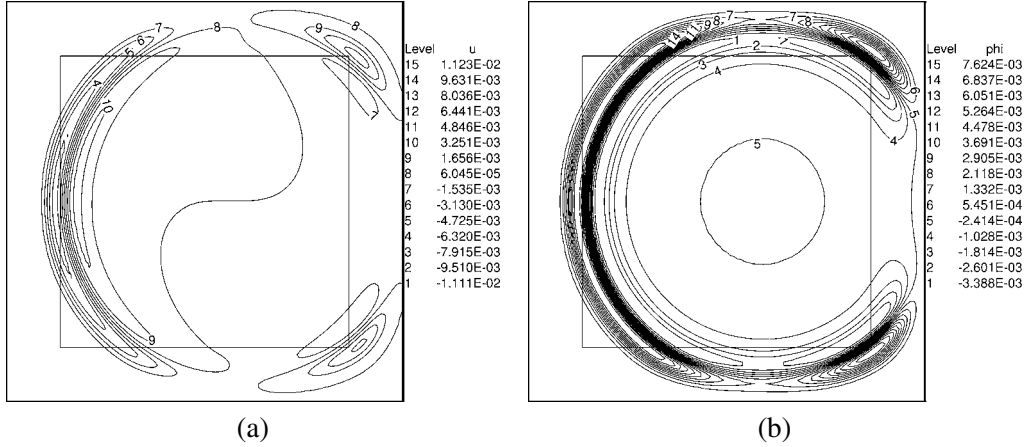
Figure 10. x-velocity (u, (a)) and potential (ϕ, (b)) contours at $t = 50$ for propagation of a Gaussian pulse at $F_0 = 0.2$, $f = 0.01$.
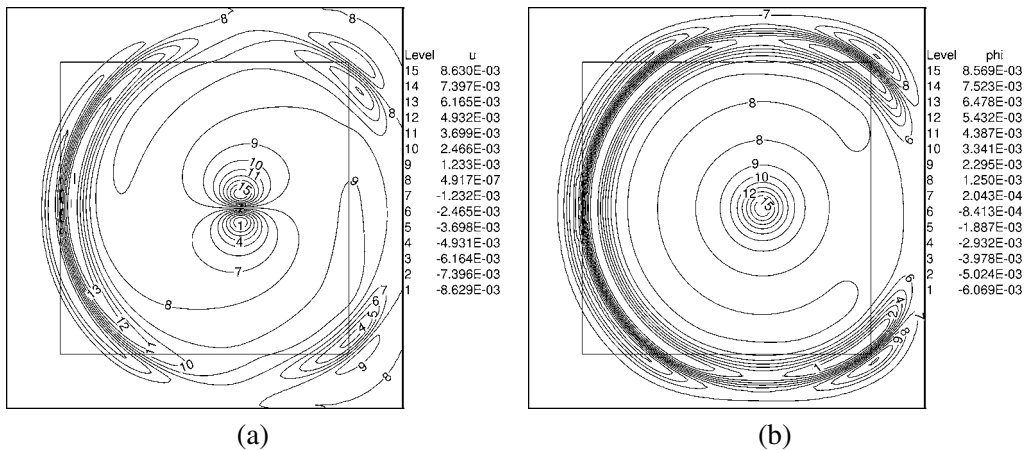
Figure 11. x-velocity (u, (a)) and potential (ϕ, (b)) contours at $t = 50$ for propagation of a Gaussian pulse at $F_0 = 0.2$, $f = 0.1$.

$t = 23$, before the pulse reaches the interior limit of the PML region, for two different values of the non-dimensional Coriolis factor $f = 0.01$ and $f = 0.1$ in a mean flow with $F_0 = 0.01$. For the results in figure 9, $F_0 = 0.2$. For this last value of the Froude number we also show, in figures 10 and 11, the contours of u and ϕ after the pulse has entered the PML domain (time $t = 50$) for $f = 0.01$, and $f = 0.1$, respectively. The effectiveness of the PML is clear from these pictures. As expected, the behavior of the maximum error at the interior limit of the PML was found to be similar to the previous cases. We note that the main effect of the Coriolis forces is, as expected, to shear and rotate the velocity field, while the potential field is hardly affected.

6. Conclusions

In all the simulations performed, the performance of Hu's newly developed PML method [14] was better than that of Abarbanel's et al. method [2]. Therefore, we recommend the former as the method of choice for lateral boundary conditions in limited-area models. Coriolis forces do not appear to affect the performance of the PML method significantly. Although we did not discuss it in this paper, we noticed that for nonlinear computations both PML methods became unstable for very long time integration. This was a consequence of nonlinear instabilities, and could be avoided by using a low-pass filter. No such instability was noticed in the linear case unless explicitly stated in the previous section.

References

[1] S. Abarbanel and D. Gottlieb, A mathematical analysis of the PML method, J. Comput. Phys. 134 (1997) 357–363.

[2] S. Abarbanel, D. Gottlieb and J.S. Hesthaven, Well-posed perfectly matched layers for advective acoustics, J. Comput. Phys. 154 (1999) 266–283.

[3] F. Alcrudo and P. Garcia-Navarro, A high-resolution Godunov-type scheme in finite volumes for the 2D shallow-water equations, Internat. J. Numer. Methods Fluids 16 (1993) 489–505.

[4] J.-P. Berenger, A perfectly matched layer for the absorption of electromagnetic waves, J. Comput. Phys. 114 (1994) 185–200.

[5] G. Darblade, R. Baraille, A.-Y. leRoux, X. Carton and D. Pinchon, Conditions limites non réfléchissantes pour un modèle de Saint-Venant bidimensionnel barotrope linéarisé, C. R. Acad. Sci. Paris 324 (1997) 485–490.

[6] C. Dawson and V. Aizinger, Upwind mixed methods for transport equations, Comput. Geosci. 3 (1999) 93–110.

[7] C. Dawson, V. Aizinger and B. Cockburn, The local discontinuous Galerkin method for contaminant transport problems, in: *Discontinuous Galerkin Methods*, eds. B. Cockburn, G. Karniadakis and C.-W. Shu, Lecture Notes in Computational Science and Engineering, Vol. 11 (Springer, New York, 1999) pp. 309–314.

[8] B. Engquist and A. Majda, Radiation boundary conditions for acoustic and elastic wave calculations, Comm. Pure Appl. Math. 32 (1979) 313–357.

[9] B. Engquist and A. Majda, Absorbing boundary conditions for the numerical simulation of waves, Math. Comp. 31 (1997) 629–651.

[10] P. Goblet and E. Cordier, Solution of the flow and mass transport equations by means of spectral elements, Water Resour. Res. 29 (1993) 3135–3144.

[11] H.E. Hayder, F.Q. Hu and M.Y. Hussaini, Towards perfectly absorbing boundary conditions for the Euler equations, AIAA Journal 37 (1999) 912–918.

[12] J.S. Hesthaven, On the analysis and construction of perfectly matched layers for the linearized Euler equations, J. Comput. Phys. 142 (1998) 129–147.

[13] F.Q. Hu, On absorbing boundary conditions for the linearized Euler equations by a perfectly matched layer, J. Comput. Phys. 129 (1996) 201–219.

[14] F.Q. Hu, A stable, perfectly matched layer for linearized Euler equations in unsplit physical variables, J. Comput. Phys. 173 (2001) 455–480.

[15] S.K. Kar and R.P. Turco, Formulation of a lateral sponge layer for limited-area shallow-water models and an extension for the vertically-stratified case, Mon. Wea. Rev. 123 (1995) 1542–1559.

[16] D.A. Kopriva and J.H. Kolias, A conservative staggered-grid Chebyshev multidomain method for compressible flows, J. Comput. Phys. 125 (1996) 244–261.

[17] E.A. Martinsen and H. Engedahl, Implementation and testing of a lateral boundary scheme as an open boundary-condition in a barotropic ocean model, Coast Engrg. 11 (1987) 603–627.

[18] I.M. Navon, B. Neta and M.Y. Hussaini, A perfectly matched layer approach to the nonlinear shallow water equations models, Mon. Wea. Rev. (submitted).

[19] B. Riviere, M.F. Wheeler and K. Banas, Discontinuous Galerkin method applied to a single phase flow in porous media, Comput. Geosci. 4 (2000) 337–349.

[20] D. Stanescu and W.G. Habashi, 2N-storage low dissipation and dispersion Runge–Kutta schemes for computational acoustics, J. Comput. Phys. 143 (1998) 674–681.

[21] C.K.W. Tam and J.C. Webb, Dispersion-relation-preserving finite difference schemes for computational acoustics, J. Comput. Phys. 107 (1993) 262–281.